Photochemical & Photobiological Sciences

ROYAL SOCIETY OF CHEMISTRY

PAPER

Cite this: *Photochem. Photobiol. Sci.*, 2020, **19**, 1344

Synthesis and photochromic behaviour of a series of benzopyrans bearing an *N*-phenyl-carbazole moiety: photochromism control by the steric effect†

Michel Frigoli, *[a] Tanguy Jousselin-Oba,[a] Masashi Mamada, [b] Jérôme Marrot,[a] Agnese Zangarelli,[c] Danilo Pannacci,[c] Chihaya Adachi [b,d] and Fausto Ortica *[c,e]

Received 28th May 2020,
Accepted 8th July 2020

DOI: 10.1039/d0pp00202j

rsc.li/pps

Five new *N*-phenyl-carbazole benzopyrans bearing different substitutions on one of the phenyl rings at the sp3 carbon have been synthesized. Their molecular structures were investigated by X-ray and NMR analyses and through quantum chemical calculations. The photochromic mechanism under UV irradiation in toluene, consisting of the consecutive formation of transoid-*cis* (TC) and transoid-*trans* (TT) isomers, was studied by UV-vis spectral and kinetic analyses. These molecules have been specifically designed to ascertain the possibility of favouring the formation of the less thermodynamically stable TT at the photostationary state, upon exploiting steric hindrance effects on the diene part of the molecule. The spectrokinetic study allowed the estimation of most of the spectrokinetic parameters, such as molar extinction coefficients, quantum yields of UV colouration and visible photobleaching, and the rate constants of the fast and slow thermal bleaching processes. Peculiar effects of substituents with different donor strengths on one phenyl ring located at the 3-position were observed on the spectrokinetic properties.

Introduction

Benzo- and naphthopyrans are well known classes of photochromic compounds[1,2] that, in consequence of their usual fatigue resistance, have received great attention over the latest years in light of their possible practical and industrial applications,[3] especially in the field of ophthalmic lens production. The mechanism of the photochromic reaction of benzo- and naphthopyrans was first investigated by Becker and coworkers[4,5] and, unlike other photochromic materials which usually display either P-Type or T-Type behaviour,[6] they exhibit a more complicated reaction mechanism. Indeed, upon steady UV irradiation, the phenomenology of these compounds can be conveniently described in terms of photoproduction of transoid-*cis* (TC) and transoid-*trans* (TT) structures[7,8] and their complete bleaching to the starting material can only be achieved by both thermal and photochemical pathways. The TC forms are more thermally labile than the TT ones, whilst their thermodynamic stability is generally higher than that of TT.[9,10] This behaviour has also been observed for the reference molecule having this skeleton, 3,3-diphenyl-3*H*-naphtho[2,1-*b*]pyran (herein named RN, Scheme 1), that has been extensively reported in the literature, especially over the last three decades.[5,7,11–27] The transformation of a benzo- or a naphthopyran into a photochromic system possessing only a T-Type or a P-Type behaviour might undoubtedly be of interest from both points of view of basic research and practical appli-

[a]*Université Paris-Saclay, UVSQ, UMR CNRS 8080, Institut Lavoisier de Versailles, 45 av des Etats-Unis, 78035 Versailles, France. E-mail: michel.frigoli@uvsq.fr*
[b]*Center for Organic Photonics and Electronics Research (OPERA), JST ERATO Adachi Molecular Exciton Engineering Project, and Academia-Industry Molecular Systems for Devices Research and Education Center, Kyushu University, Kyushu University, Nishi, Fukuoka, 819-0395 Japan*
[c]*Dipartimento di Chimica, Biologia e Biotecnologie, Università degli Studi di Perugia, Via Elce di Sotto 8, 06123 Perugia, Italy. E-mail: fausto.ortica@unipg.it*
[d]*International Institute for Carbon Neutral Energy Research (WPI-I2CNER), Kyushu University, Nishi, Fukuoka 819-0395, Japan*
[e]*Istituto Nazionale di Fisica Nucleare (INFN), Sezione di Perugia, Via Pascoli, 06123 Perugia, Italy*

†Electronic supplementary information (ESI) available. CCDC 1998515. For ESI and crystallographic data in CIF or other electronic format see DOI: 10.1039/d0pp00202j

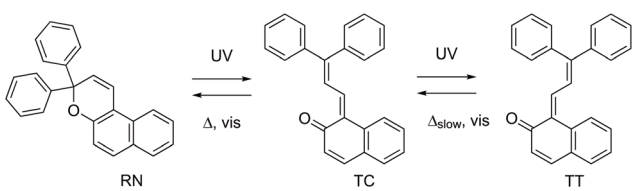

Scheme 1 Mechanism of the photochromic reaction of 3,3-diphenyl-3*H*-naphtho[2,1-*b*]pyran.

cations. This could be achieved by choosing a suitable solvent, the temperature range or introducing modifications of the molecular structure.

On the one hand, a fully thermoreversible photochromic naphthopyran might be interesting in the realization of fast responsive optical switches while, on the other hand, a completely photoreversible molecule could be useful to produce bistable devices and systems for optical storage. Some examples have been recently reported in the literature, especially on the possibility to transform naphthopyrans into thermally reversible compounds, by substituting the pyran ring with a furan one[28,29] or the synthesis of fused-naphthopyrans[30,31] or through an on-demand control of the photochromic properties, achieved by increasing the ring-size of the alkylenedioxy moiety on the naphthopyrans.[32]

One alternative approach, based on the attempt to synthesize a prevalently photoreversible naphthopyran, has been reported by one of us, carried out through the control of the photochromism of naphthopyran derivatives by means of intramolecular CH–π bonds.[33] Indeed, the photochromism of naphthopyran was shown to be under thermodynamic control. In the framework of this project, we also reported afterwards some studies on helicene-naphthopyrans,[34,35] confirming that the improvement of the thermodynamic stability of the TT isomers, compared to the TC ones, played an important role in increasing the spectrokinetic contribution of the TT to the overall mechanism of the photochromic reaction, along with a reduced importance of the TC role at the photostationary state. In both cases mentioned above, even though TT was more thermodynamically stable than TC, we could argue that the return from TT to TC then to CF through isomerization of one double bond was made more difficult due to the steric hindrance of the helical part of the photochrome on the dienic moiety. One question is raised: is it possible to favour the formation of TT compared to TC at the photostationary state while TT is less thermodynamically stable than TC just by crowding the diene part of the molecule?

Herein, we have specifically designed a photochromic system, namely 3,3,13-triphenyl-3,13-dihydrochromeno[5,6-*a*] carbazole (CN-Ph-H), to respond to the above question and prepared some derivatives for which one phenyl group located at the 3-position was systematically functionalised with different donor groups, such as di(pyridin-2-yl)amine (CN-Ph-N(Py)$_2$), diphenylamine (CN-Ph-N(Ph)$_2$), methoxy (CN-Ph-OMe) and dimethylamine (CN-Ph-N(Me)$_2$), as shown in Fig. 1, in order to study their impacts on the spectrokinetic properties and more specifically to see whether there is any relationship between the rate constants of bleaching of TC and TT.

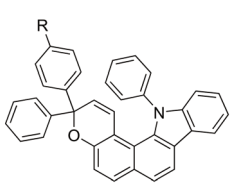

R: H, OMe, N(Pyridyl)$_2$, N(Phenyl)$_2$, N(Methyl)$_2$

Fig. 1 Molecular structure of the *N*-phenyl carbazole benzopyrans (CN-Ph-R).

Experimental

General methods for synthesis

All reactions were carried out under argon. Dichloromethane was distilled from P_2O_5, and THF and toluene were distilled over Na/benzophenone. Dichloromethane and toluene were kept over activated 3 Å molecular sieves. 1,2-Dichloroethane was dried over activated 3 Å molecular sieves. All commercial reagents were used without further purification. ^{1}H and ^{13}C NMR spectra were recorded at room temperature on a Bruker Avance-300 MHz NMR spectrometer. ^{1}H NMR spectra were recorded at 300 MHz and ^{13}C NMR spectra were recorded at 75 MHz. Chloroform residual peak was taken as the internal reference at 7.26 ppm for ^{1}H NMR and 77 ppm for ^{13}C NMR. Acetone residual peak was taken as the internal reference at 2.09 ppm for ^{1}H NMR and 205.87 ppm for ^{13}C NMR. DMSO residual peak was taken as the internal reference at 2.54 ppm for ^{1}H NMR and 40.45 ppm for ^{13}C NMR. High-resolution mass spectra were obtained by using a Waters Xevo Q-Tof using positive mode. Infrared spectra were recorded from a Nicolet 6700 FT-IR spectrometer.

Instruments and methods

UV-vis absorption spectra were recorded on a PerkinElmer Lambda 800 double-beam spectrophotometer. For monitoring the spectral modifications of the molecules in real time under either UV or visible irradiation, an HP 8453 diode-array spectrophotometer was used. Photoreaction measurements were carried out in toluene (purchased from Merck, spectrophotometric grade, used as received) in a 1 cm-path cell in the spectrophotometer holder with the irradiating and the probe beams forming a right angle. A 125 W xenon lamp, coupled with a Jobin–Yvon H10 UV monochromator for the wavelength choice and a fibre-optic system, was employed as the irradiation source for the photoreaction studies. The quantum yields of the photocolouration and photobleaching processes were determined by spectrophotometry, using potassium ferrioxalate actinometry to measure the radiation intensity, typically of the order of 5×10^{-6} moles of photons per dm^3 per s.

Fluorescence measurements were recorded on a Spex Fluorolog-2 1680/1 instrument, equipped with a system for spectral correction; the quantum yields were determined by using quinine sulphate in 1N H_2SO_4 (quantum yield $\phi_F = 0.546$ (ref. 36)) as the standard. The corrected areas of the sample and the standard emissions were compared by using eqn (1), which accounts for the differences in absorbance and refraction index of the sample (A_F and n_F) and standard (A_{St} and n_{St}) solutions.

$$\phi_F = \phi_{St} \frac{(\text{Area})_F}{(\text{Area})_{St}} \frac{A_{St}}{A_F} \frac{{n_F}^2}{{n_{St}}^2} \quad (1)$$

Sample concentrations were always adjusted to keep the absorbance below 0.1. The accuracy in the ϕ_F values is estimated to be within 10%.

X-Ray diffraction (XRD) analysis was conducted on a single-crystal diffractometer Bruker AXS X8 APEX I using Mo radiation.

For the HPLC analysis, either a Gemini C18, 5 μm, 4.6 × 150 mm column or a Prontosil 200-3-C30, 3 μm, 4.6 × 150 mm column was alternatively used on a Waters HPLC facility, equipped with a Waters 600 controller and a Waters 996 photodiode array detector. Pure acetonitrile or an acetonitrile/water mixture up to 95/5 volume ratio was used as the eluent.

Results and discussion

Synthesis

The synthesis of the photochromic materials relies first on the preparation of 11-phenyl-11*H*-benzo[*a*]carbazol-2-ol, which was obtained in two steps from the known 2-methoxy-11*H*-benzo[*a*]carbazole, as depicted in Scheme 2.[37] The first step was an *N*-arylation of the carbazole moiety using the catalyst derived from CuI and *trans*-1,2-cyclohexanediamine as proposed in 2002 by Buchwald and co-workers. Under these conditions, an *N*-arylated product, compound **2**, was obtained in 80% yield.[38] The second step was a simple demethylation using boron tribromide as the demethylation agent and the desired product was prepared in 95% yield.

The introduction of 2,2′-dipyridylamine and diphenylamine in one phenyl of the photochromic materials leads to the preparation of the ketones **4** and **5** respectively, which were obtained by using the Ullmann condensation between 4-bromobenzophenone and the corresponding amine (Scheme 3). The reaction worked well with 2,2′-dipyridylamine since the corresponding ketone **4** was obtained in 80% yield. The ketone 5 functionalised with diphenylamine was obtained in only 33% yield.[39]

From commercially available 4-methoxybenzophenone and 4-dimethylaminobenzophenone and the benzophenones **4** and **5**, the corresponding propargylic alcohols were prepared by the addition of the lithium-trimethylsilylacetylene on the benzophenone, followed by the cleavage of the trimethylsilyl group with an excess of potassium carbonate in MeOH/THF, as shown in Scheme 4. Then, the condensation between compound **3** and commercially available 1,1-diphenylprop-2-yn-1-ol or the propargylic alcohols **6–9** provided the desired photochromic materials (Scheme 4).

X-ray analysis

A suitable monocrystal of CN-Ph-H for X-ray analysis was obtained. The crystals have a monoclinic symmetry with a *C*2/*c*

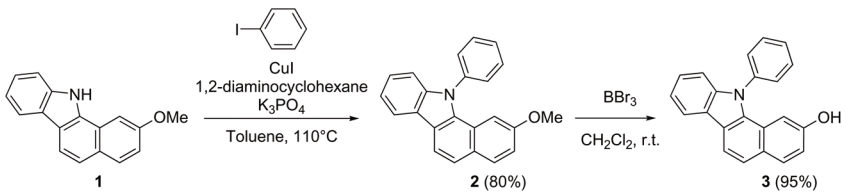

Scheme 2 Preparation of 11-phenyl-11*H*-benzo[*a*]carbazol-2-ol.

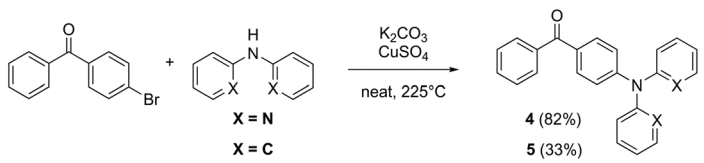

Scheme 3 Preparation of 2,2′-dipyridylamine- and 2,2′-diphenylamine-benzophenones.

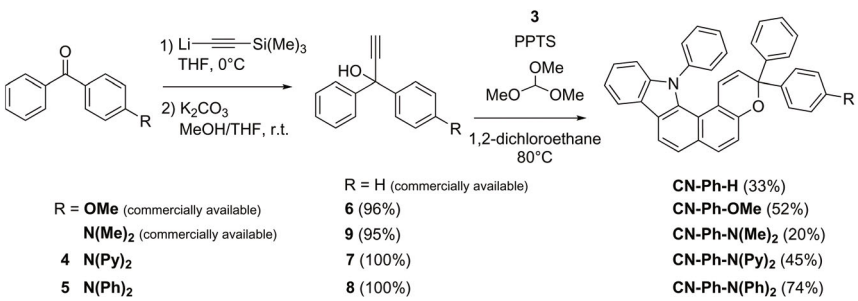

Scheme 4 Final steps in the synthesis of the photochromic materials.

space group. Two enantiomers are present in the crystals. They differ in the position of the phenyl ring C compared to the chromene ring of the molecule. In Fig. 2a, the ring C is behind the chromene ring. The molecule is stabilized with three hydrogen bonds. There is a CH–π interaction between proton 3″ and the ring C. The geometry of the edge-to-face interaction is as follows: the distance between the proton and the ring centroid of the ring C is 3.228 Å and the dihedral angle between the interacting ring planes is 53.44°. A CH–O bond between proton 3′ and oxygen 4 is observed with a distance of 2.308 Å and the angle between C–H3′ and O4 is 102.81°. There is also a CH–N bond between proton 1 and the nitrogen 13 with a distance of 2.583 Å and the angle between C–H1 and N14 is 120.83°. The distance between protons 1 and 2 is 1.318 Å, which is typical of a localized double bond. The dihedral angle between the two planes formed by the two phenyl rings A and B is 77.92°. It should be noted that for the TC form, ring A is slightly less twisted with the diene part of the molecule compared to ring B whereas for TT, it is ring B which is less twisted. Actually, the phenyl group facing the proton is more planar.

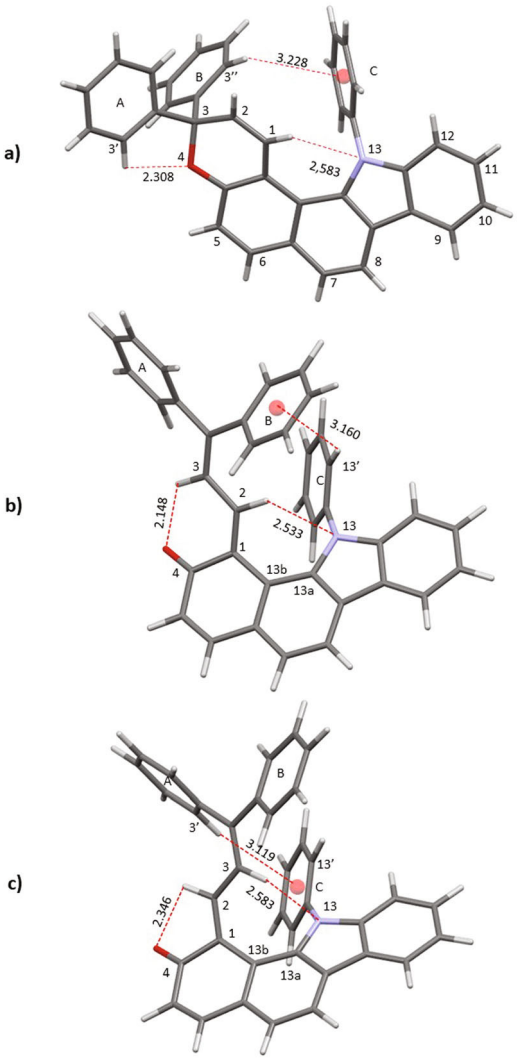

Fig. 2 (a) X-ray structure of CN-Ph-H; optimized structures at CAM-B3LYP of (b) the TC form and (c) TT form.

Thermodynamic stability

So far, P-type photochromism based on [3*H*]-naphthopyran was observed for systems in which the TT form was more thermodynamically stable than the TC form. Therefore, theoretical calculations were performed at the CAM-B3LYP/6-31G(d,p) and M06-2X/6-31G(d,p) levels of theory since they are optimized to reproduce well weak interactions that are essential in the investigated compound, and compared with the reference [3*H*]-naphthopyran (RN) (see Table 1).

For RN and CN-Ph-H, the closed form is the most thermodynamically stable, followed by the TC form, and then by the TT form, whatever the level of theory. As shown in Fig. 2(b) and (c), TC and TT are stabilized by at least three hydrogen bonds as for the closed form. As for RN, TT is less thermodynamically stable than TC because the diene part of the molecule interacts less with the rest of the molecule. Indeed, the dihedral angle between carbons 2 and 13a is 41.62° for TT, larger than that of TC for which the dihedral angle is 31.45°. This difference also explains why TT absorbs at lower wavelengths than TC. Since RN is known to display T-type photochromism in solution, would it be the same for CN-Ph-H and the other derivatives?

Photochromic properties

The quantitative absorption spectra of the five CN-Ph benzopyrans in toluene are shown below (Fig. 3). All compounds exhibit similar features showing a structure that is probably due to at least two different electronic transitions. The small differences are related to the changes in the substituent on one of the benzene rings located in the 3-position. The absorption spectra of the photochromes correspond nearly to the sum of the naphthopyran core and the substituted phenyl at the 3 position.

Table 1 Relative Gibbs free energies [kcal mol^{-1}] in toluene computed by using DFT for the different systems under investigation. All values were calculated by using the most stable isomer, CF, as a reference

Compound	CF	TC		TT		TT–TC	
Level of theory	—	CAM-B3LYP	M06-2X	CAM-B3LYP	M06-2X	CAM-B3LYP	M06-2X
RN	0	8.39	11.41	9.55	12.21	1.16	0.80
CN-Ph-H	0	6.74	9.67	8.29	10.62	1.55	0.95

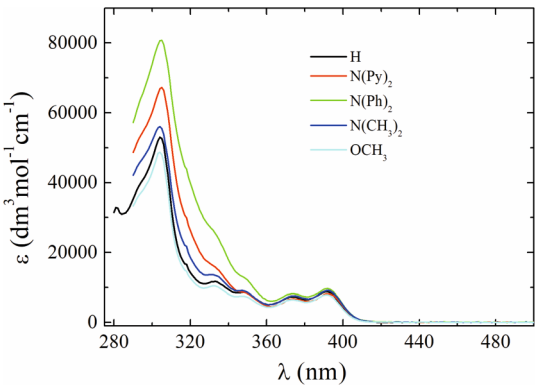

Fig. 3 Quantitative absorption spectra of the five *N*-phenyl carbazole benzopyrans in toluene.

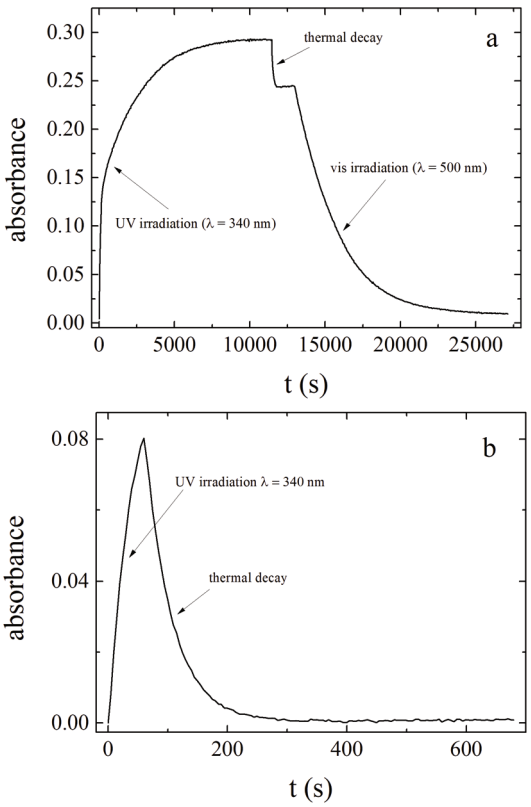

Fig. 4 Kinetic profile monitored at 500 nm for CN-Ph-H obtained upon (a) consecutive UV irradiation at λ = 340 nm, thermal decay and final visible decolouration at λ = 500 nm; (b) short UV irradiation at λ = 340 nm, followed by complete thermal bleaching.

CN-Ph-H. When a toluene solution containing one of the *N*-phenyl carbazole benzopyrans is exposed to UV light, a common trend is observed for the five molecules. Upon UV irradiation, an initial steep rise of absorbance in the visible region is followed by a longer-lived further increase, up to the attainment of a photostationary state. The kinetic behaviour of the photocolouration curve, characterized by a clear biexponential trend, is shown in Fig. 4a for CN-Ph-H. Once the UV irradiation is interrupted, a fast thermal decay occurs, along with a rapid decrease of the absorbance in the visible region, which stops after a few hundreds of seconds (second part of the kinetics in Fig. 4a). The residual colouration only bleaches if visible irradiation is carried out, up to a complete fading of the colour (third part of the kinetics in Fig. 4a). Otherwise, if the coloured chromene is kept in the dark after the fast thermal decay following the attainment of the photostationary state and it is not subjected to any kind of further irradiation, it undergoes a very slow thermal decolouration, which only becomes barely perceptible after a few months (Fig. S3†).

In addition to that, when the solution containing the chromene was only exposed to UV light for a short time, usually about a hundred of seconds, and then its thermal decay was monitored once the irradiation had been discontinued, a complete rapid decolouration of the system was observed (Fig. 4b).

The decay rate constants for both the "fast" and the "slow" processes, obtained through a first order treatment of the kinetics, are reported in Table 3. The foregoing results can be explained in terms of the following reaction scheme (Scheme 5), which is based on the aforementioned experimental data and on results previously reported in the literature on similar naphthopyrans.[33–35,40]

Based on this reaction mechanism, the initial chromene, in its closed colourless form, upon UV irradiation is transformed through a consecutive 2-step reaction into a transoid-*cis* open coloured isomer (TC) which in turn, upon prolonged irradiation, eventually evolves into the more thermally stable transoid-*trans* open coloured isomer (TT). The latter is responsible for the residual colouration that persists over months if the system is kept stored in the dark and bleaches completely to the starting material upon visible irradiation. This reaction mechanism is further supported by the short irradiation experiment reported in Fig. 4b, where the thermally unstable TC open isomer, immediately formed upon UV photocolouration, does not further evolve into the TT form once the irradiation is interrupted, but undergoes thermal bleaching up to a complete fading. Indeed, after a prolonged UV irradiation,

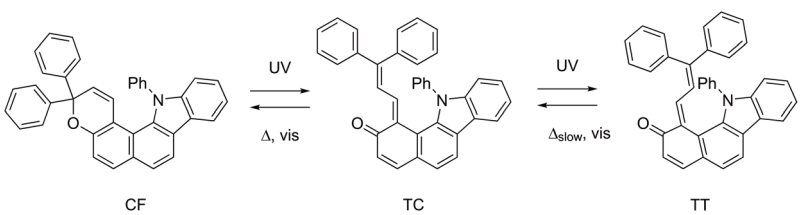

Scheme 5 Mechanism of the photochromic reaction, showing the chromene (CF) and the main coloured isomers, transoid-*cis* (TC) and transoid-*trans* (TT).

upon injection of the solution containing the photostationary state mixture of CN-Ph-H into the HPLC column, only two peaks were revealed, related to the residual initial chromene and the TT isomer, respectively. Owing to its relatively fast thermal decolouration process, the presence of the TC species could not be detected in the chromatogram.

In the light of all these findings, HPLC separation of the photostationary state mixture allowed the pure TT isomer to be collected. The complete quantitative absorption spectrum of the TT isomer could then be obtained upon selecting a wavelength where only very slight absorbance changes under irradiation are observed and setting the TT molar extinction coefficient equal to that of the initial closed form at that wavelength. A more precise approach would be that based on the use of a real isosbestic point that however, in the present case, owing to the mechanism of the reaction involving three different species, could not be detected. The quantitative absorption spectrum of the TT isomer of CN-Ph-H is displayed in Fig. 5.

An algorithm was then used to determine also the quantitative absorption spectrum of the TC isomer. After UV irradiation, followed by HPLC separation, the TT concentration could be obtained by means of the ε_{TT}, evaluated according to the aforementioned procedure, and the absorbance value of the kinetic profile at 500 nm, measured after the thermal decay following the photostationary state had occurred. This would also allow the evaluation of the conversion % of the starting molecule into the TT isomer. Then, considering the ratio between the peak areas of the closed form and the TT open isomer observed in the HPLC once the TC decay is complete, at a wavelength that best approximates the isosbestic point, the following relation holds:

$$\frac{\text{Area}_{TT}}{\text{Area}_{\text{colourless}}} = \frac{[TT]}{[\text{colourless}']} \quad (2)$$

Therefore, the concentration of the closed form after the complete TC thermal decay, [colourless′], could be determined. The absorbance decrease at 500 nm on going from the photostationary state to the complete decay of the TC species is correlated with the corresponding increase in the colourless form concentration originating from the TC thermal bleaching; therefore:

$$\frac{[\text{colourless}'] - [\text{colourless}'']}{[\text{colourless}'']} = \frac{A''_{500\,\text{nm}} - A'_{500\,\text{nm}}}{A''_{500\,\text{nm}}} \quad (3)$$

where the prime symbol refers to the situation after the TC thermal decay has occurred, while the second one is related to the photostationary state. Once the concentration of the closed form at the photostationary state, [colourless″], has been determined from (3), the concentration of the TC isomer can be evaluated, and the molar extinction coefficient of the TC isomer at a particular wavelength can be derived:

$$[TC] = [\text{colourless}'] - [\text{colourless}''] \quad (4)$$

$$\varepsilon_{TC}^{500} = \frac{A''_{500\,\text{nm}} - A'_{500\,\text{nm}}}{[TC]} \quad (5)$$

However, once the TC concentration has been obtained (eqn (4)), one can subtract the contributions of the CF and the TT species from the total absorption spectrum at the photostationary state, using their quantitative spectra and their concentrations at the photostationary state itself ([colourless″] and [TT]). The complete quantitative spectrum of the TC isomer can then be derived and it is shown in Fig. 5. The contribution of the TC isomer is clearly higher at longer wavelengths, as expected from the literature.

As clearly visible from the first part of the kinetic profile in Fig. 4a, the UV photocolouration kinetics of the CN-Ph molecules exhibit a biexponential behaviour, as expected in such systems characterized by a consecutive three-step reaction mechanism. A complete quantitative treatment to provide the quantum yields of all the reaction steps involved, by solving the kinetic equations in a rigorous way, is practically impossible in this situation.[8] However, if one takes into account only the early instants of the UV irradiation, when only the TC isomer is substantially formed, as also pointed out by the short irradiation tests, the initial rate method is helpful to obtain the quantum yield ϕ for the conversion of CF into TC:

$$\frac{\Delta A_{TC}}{\Delta t} = \varepsilon_{TC}\phi_{CF\rightarrow TC}I^0(1 - 10^{-A'_{TC}}) \quad (6)$$

In eqn (6), the first term refers to the finite variation of absorbance in the early time interval of the UV irradiation kinetics, and therefore corresponds to the formation of the TC coloured isomer. ε_{TC} is the molar extinction coefficient of the TC, $\phi_{CF\rightarrow TC}$ is the quantum yield of TC formation, A'_{TC} is the total absorbance at the irradiation wavelength and I^0 is the intensity of the irradiation light, determined by chemical actinometry. Once the ε_{TC} at the wavelength where the kinetics has been recorded is known, the quantum yield value of TC formation from the initial closed form, $\phi_{CF\rightarrow TC}$ = 0.43, could be obtained (Fig. S4†).

Even though the TT isomer exhibits a notable thermal stability in the dark at room temperature in toluene solution,

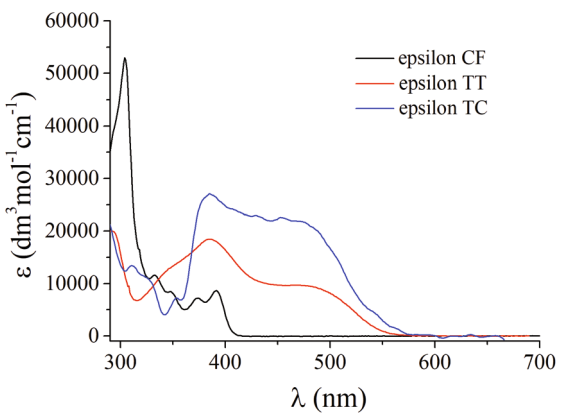

Fig. 5 Quantitative absorption spectra of the TC and TT coloured isomers obtained upon UV irradiation of CN-Ph-H in toluene.

its transformation to the CF *via* TC can be accelerated by means of visible light irradiation. In our case, the CN-Ph-H was irradiated at 435 nm, and the corresponding photobleaching kinetics at 500 nm was recorded (Fig. 6).

The TT absorption signal follows a first order decay and a procedure similar to that already employed to determine the quantum yield of UV photocolouration can also be used for visible photodecolouration data treatment, by taking into account the first experimental points of the bleaching kinetics, where only the TT isomer significantly contributes to the total absorbance:

$$\frac{\Delta A_{TT}}{\Delta t} = \varepsilon_{TT}\phi_{TT\rightarrow CF}I^0(1 - 10^{-A'_{TT}}) \quad (7)$$

In eqn (7), ε_{TT} is the molar extinction coefficient of the TT, $\phi_{TT\rightarrow CF}$ is the quantum yield of visible photobleaching, A'_{TT} is the total absorbance at the irradiation wavelength and I^0 is the intensity of the irradiation light, determined by chemical actinometry. The value of the quantum yield of visible irradiation, $\phi_{TT\rightarrow CF}$, is reported in Table 3. Finally, as previously mentioned, from the concentration value of the TT isomer, determined after the complete thermal decay of the TC following the photostationary state attainment, the percentage of transformation of the initial chromene into the stable coloured form could be calculated (Table 3).

CN-Ph-R. The photobehaviour of the four substituted molecules (CN-Ph-R, with R = –OMe, –N(methyl)$_2$, –N(phenyl)$_2$ and –N(pyridyl)$_2$) is substantially similar to that of the unsubstituted compound (CN-Ph-H). The UV photocolouration was characterized by a biexponential trend, and once the photostationary state had been attained, interruption of the irradiation only caused a partial bleaching of the system, and the residual colouration persisted throughout several weeks. Full decolouration was only achieved upon visible irradiation of the solution with complete restoration of the initial chromene. However, unlike CN-Ph-H, when the solution at the photostationary state was injected into the HPLC column, three peaks were observed instead of two, corresponding to three different thermally stable molecules, as shown in Fig. 7 for CN-Ph-OMe.

One signal corresponds to the residual initial chromene present at the photostationary state, while the other peaks refer to two different thermally stable TT isomers produced upon UV irradiation, as clearly indicated by the spectral features observed for the two peaks at the diode array detector of the HPLC. Indeed, in the case of the CN-Ph-R compounds, the presence of a substituent on one of the phenyl rings on the sp^3 carbon gives rise to two different transoid-*trans* isomers upon UV photocolouration, namely the *cis*-transoid-*trans* (CTT) and the *trans*-transoid-*trans* (TTT); the latter formed through the corresponding transoid-*cis* isomers (CTC and TTC) (Scheme 6).

HPLC analysis allowed the two TT coloured isomers to be separated and then selectively irradiated by visible light to study their photobleaching behaviour. The photodecolouration from TT to CF occurred through a clear pathway and the presence of an isosbestic point allowed the measurement of the quantitative spectra of the stable TT coloured isomers, using the same procedure already described for CN-Ph-H. The quantitative absorption spectra of the TT isomers are displayed in Fig. 8, while their absorption maxima are collected in Table 2, along with the normalized absorption and TC/TT absorption ratio at the photostationary state. The ratios between CTT and TTT are different between OMe and the couple of N-(Py)$_2$ and N-(Ph)$_2$ derivatives. This can be explained by the contribution of the lone pair in the π-conjugation of the heteroatom in anisole and triphenylamine groups. The oxygen in anisole has an sp^3 hybridization and therefore the lone pair of oxygen makes an angle of 120° with the phenyl, whereas, in triphenylamine, the nitrogen is more planar, with nitrogen-torsion angles varying between *ca.* 160 and 180°, indicating that the lone pair of nitrogen is more involved in the π-conjugated system.[41] Since ring B in TTT is slightly less twisted than ring A (see Fig. 2), the lone pair of the groups is slightly more involved in the whole π-conjugated system when the group is

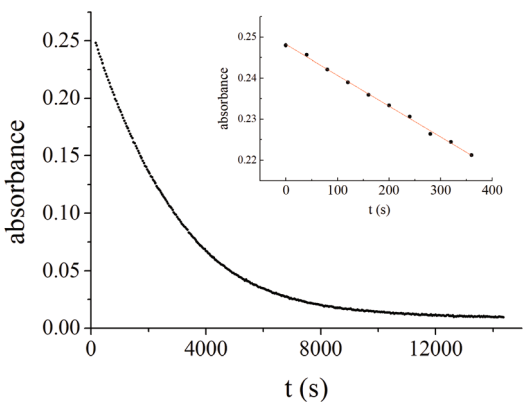

Fig. 6 Kinetics of visible photobleaching (λ_{irr} = 435 nm) of CN-Ph-H in toluene, monitored at 500 nm. Inset: linear interpolation of the first points of the decay (see below).

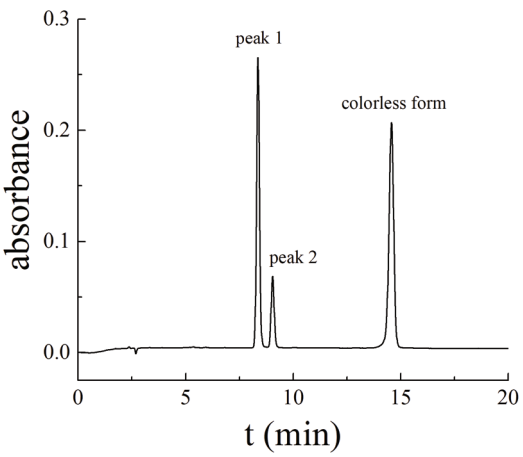

Fig. 7 Chromatogram obtained at the HPLC upon injection of a solution of CN-Ph-OCH$_3$ in toluene, after UV irradiation until attainment of the photostationary state.

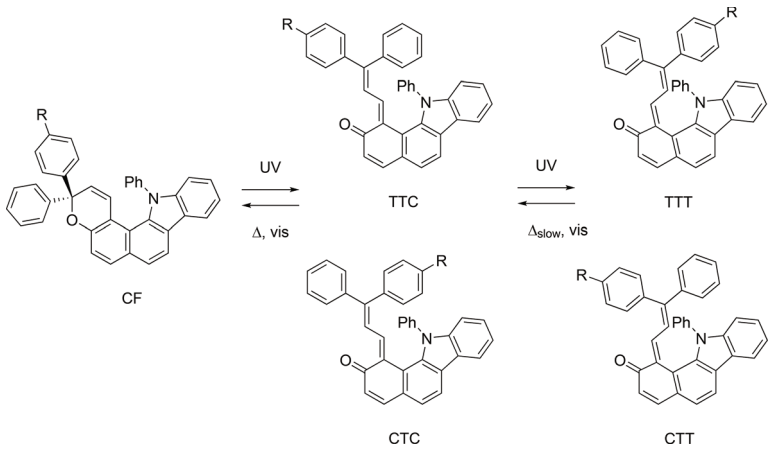

Scheme 6 Mechanism proposed for the photochromic reaction of the CN-Ph-R chromenes, showing the initial closed form (CF) and the main coloured transoid-*cis* (CTC and TTC) and transoid-*trans* (CTT and TTT) isomers.

attached to ring B, favouring the formation of the TTT form. The effect is more pronounced when the nitrogen group is involved since the lone pair of the nitrogen is more implicated in the π-conjugation.

CN-Ph-H has an absorption maximum (λ_{max}) at 471 nm which is bathochromic shifted by 15 nm and 19 nm for CN-Ph-OMe (486 nm) and CN-Ph-N(pyridyl)$_2$ (490 nm), respectively. Larger bathochromic shifts of 47 nm and 62 nm are observed for CN-Ph-N(phenyl)$_2$ (518 nm) and CN-Ph-N(methyl)$_2$ (533 nm) respectively. Indeed, the λ_{max} is related to the HOMO–LUMO level, which in turn is mainly due to the oxidation potential of the substituent (HOMO) as the acceptor part of the molecule is the same.

The colourability defined as the absorbance reached at the PS state is the same for all compounds (around 1) except for CN-Ph-N(methyl)$_2$ which is slightly less important (0.84). At the PS state, the absorption contribution of the TC form (15.8%) for CN-Ph-H is less important than that obtained for CN-Ph-OMe (23.1%). For CN-Ph-N(pyridyl)$_2$ and CN-Ph-N(phenyl)$_2$, the absorption contribution of the TC form increases to around 30% and increases even further for CN-Ph-N(methyl)$_2$ to 38%.

As can be inferred from Fig. 8, the molar extinction coefficients of each pair of TT isomers for a given molecule exhibit values of the same order of magnitude, even though the amounts formed upon irradiation are different (see Fig. 7 for CN-Ph-OMe). This is clearly visible for CN-Ph-N(pyridyl)$_2$ and the aforementioned CN-Ph-OMe. In the case of CN-Ph-N(phenyl)$_2$ the unbalance between the two TT coloured forms was so large that the area of one of the two peaks was only barely perceptible (less than 1% of the total signal of the coloured isomers). Therefore, it was possible to isolate only one of the two TT isomers to perform its selective photobleaching experiment and record its quantitative absorption spectrum. Irradiation of CN-Ph-N(methyl)$_2$ did not allow any of the two TT species to be isolated at the HPLC, due to their relatively fast thermal decay. The different behaviour of this compound originates only from the stronger electronic effect of the substituent, since the steric hindrance is substantially the same for all the molecules investigated. In consequence, it was not possible to measure the quantitative absorption spectra of the TT isomers and only a spectrum at the photostationary state, including of course the residual closed form and the TT coloured species, could be reported (Fig. 8d). For all compounds, the major TT photoproduct eluates first using silica-C18 as a non-polar stationary phase, indicating that the same photoisomer is produced in larger quantity and corresponds to the more polar product. Theoretical calculations indicate that TTT has a dipolar moment higher than CTT (see Table S3 in the ESI†). Therefore, TTT is likely to be the most abundant species produced at the PS state. According to theoretical calculations, TTT should also have a slightly higher molar extinction coefficient than CTT, confirming that peak 1 corresponds to the TTT isomer.

The visible photobleaching reaction was also performed at 435 nm for each separated TT isomer, using potassium ferrioxalate as a chemical actinometer. The same procedure based on the initial rate method, already employed for the TT form of CN-Ph-H (eqn (7)), was then used to measure the visible photobleaching quantum yield, $\phi_{TT\rightarrow CF}$, of the various TT isomers isolated at the HPLC for the CN-Ph-R molecules. The values are collected in Table 3.

The percentage of transformation of the initial colourless chromene into the stable TT isomers was also measured through the analysis of the chromatographic traces at a suitable wavelength where the absorbance values of all the species involved (CF and the two TTs) were easily measurable. By taking into account the molar extinction coefficients of the CF and the TT coloured species and the peak areas, the % values of the stable TT isomers formed could be calculated (Table 3).

When the thermally stable TT isomers were not subjected to visible irradiation, their residual colour faded in the dark, at room temperature, over relatively long times. However, the rate constants for this thermal bleaching process exhibited a

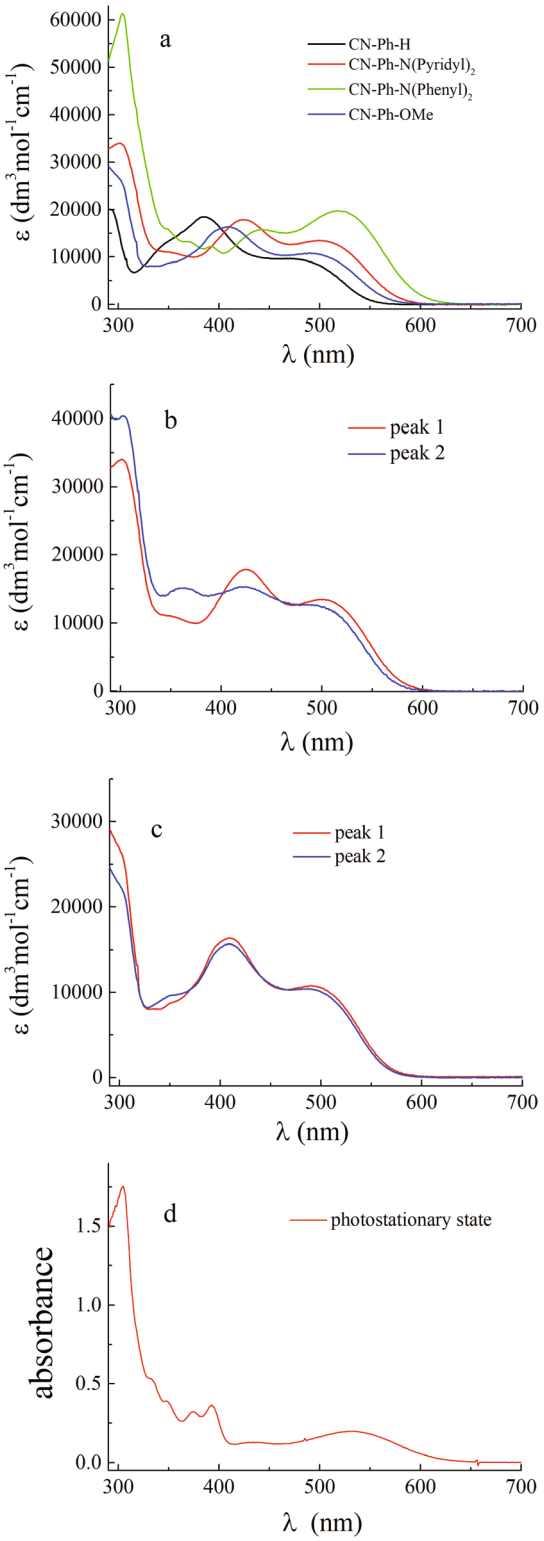

Fig. 8 (a) Quantitative absorption spectra of the TTT (peak 1, see the text below) forms produced upon irradiation of the CN-Ph-R molecules, along with that of the TT obtained for the unsubstituted CN-Ph-H; the two TTT (peak 1) and CTT (peak 2, see text) coloured isomers produced upon irradiation of CN-Ph-N(pyridyl)$_2$ (b) and CN-Ph-OMe (c); (d) absorption spectrum of the photostationary state mixture obtained upon irradiation of CN-Ph-N(methyl)$_2$.

Table 2 Absorption maxima (λ_{max} (nm)) of the TT isomers obtained upon UV irradiation of the CN-Ph molecules at 340 nm; absorption at the photostationary state measured at the longest wavelength in the visible region ($A^{max}_{PSS}/A'_{340\ nm}$) and at 500 nm ($A^{500}_{PSS}/A'_{340\ nm}$) normalized to the initial absorbance of the CF at the irradiation wavelength (340 nm); TC/TT absorption ratio at the photostationary state measured at the longest wavelength in the visible region ($A\%^{max}_{TC/TT}$) and at 500 nm ($A\%^{500}_{TC/TT}$)

	λ_{max} (nm)		$A^{max}_{PSS}/A'_{340\ nm}$	$A\%^{max}_{TC/TT}$	$A^{500}_{PSS}/A'_{340\ nm}$	$A\%^{500}_{TC/TT}$
–H	345(sh); 384; 471		1.01	15.8	0.95	15.8
–N(pyridyl)$_2$	350; 424; 498	363; 422; 490	1.02	29.5	1.02	29.5
–N(phenyl)$_2$	392; 443; 518		1.00	28.7	0.92	28.6
–OMe	350; 410; 490	350; 410; 486	1.04	23.1	1.03	23.1
–N(methyl)$_2$	435; 533		0.84	38.0	0.67	37.1

certain dependence on the kind of substituent present on one of the phenyl rings on the sp3 carbon of the chromene structure (Table 3). Decay rate constants ranged from the order of 10^{-8} s^{-1}, as in the cases of CN-Ph-H (Fig. S5a†) and CN-Ph-N(pyridyl)$_2$, to 10^{-4} s^{-1} for CN-Ph-N(methyl)$_2$ (Fig. S5b†).

From the data in Table 3, it can be seen that the rate constant of the back reaction from TC to CF ($k_{\Delta 1}$) is similar for CN-Ph-H and CN-Ph-N(pyridyl)$_2$ even though the latter absorbs at longer wavelengths (see Fig. 8 and Table 2). $k_{\Delta 1}$ increases twice when the *N*-dipyridyl group (0.018 s^{-1}) is changed to *N*-diphenyl (0.035 s^{-1}) and increases four times when dimethylamine (0.068 s^{-1}) is used. Clearly, increasing the donor strength reduces the stability of the TC form. Surprisingly, $k_{\Delta 1}$ of CN-Ph-OMe (0.042 s^{-1}) is similar to that of CN-Ph-N(phenyl)$_2$ (0.035 s^{-1}), indicating that methoxy and diphenylamine groups have a similar electronic effect. This result is very interesting since the diphenylamine group allows the shift of the absorption behaviour by 32 nm in comparison with a methoxy functionalisation, while the rate constants are similar for both groups. The same trend as that obtained for $k_{\Delta 1}$ is observed for the rate constant of the back reaction from TT to CF ($k_{\Delta 2}$). It is worthwhile to notice that upon increasing $k_{\Delta 1}$ by a factor of 2 between CN-Ph-N(pyridyl)$_2$ and CN-Ph-N(phenyl)$_2$, $k_{\Delta 2}$ increases by two orders of magnitude. In a similar manner, upon increasing $k_{\Delta 1}$ by 4 between CN-Ph-N(pyridyl)$_2$ and CN-Ph-N(methyl)$_2$, $k_{\Delta 2}$ increases by four orders of magnitude. These results indicate that the electronic effect is much more pronounced on the stability of the TT form than that of the TC form. The photochemical quantum yield from TTT to CF follows the same trend as that obtained for $k_{\Delta 1}$. For the percentage conversion from CF to TT derivatives obtained at the PS state, CN-Ph-H presents the highest conversion of 64%. Even though the stability of the photoproducts of CN-Ph-N(pyridyl)$_2$ is similar to that of CN-Ph-H, the conversion ratio is only 44%. The reduced conversion ratio is due to the presence of TC forms in a larger quantity at the PS state (see Table 2). Decreasing the thermal stability of the photoisomers

Table 3 Percentage of TT formation from CF, quantum yields of TT visible photobleaching and decay rate constants for the thermal bleaching processes of TC ($k_{\Delta 1}$) and TT ($k_{\Delta 2}$) isomers

	$\%_{CF\rightarrow TT1}$	$\%_{CF\rightarrow TT2}$	$\phi_{TT1\rightarrow CF}$	$\phi_{TT2\rightarrow CF}$	$k_{\Delta 1}$ (s^{-1})	$k_{\Delta 2(TT1)}$ (s^{-1})	$k_{\Delta 2(TT2)}$ (s^{-1})
H	64		0.010		0.022	3.9×10^{-8}	
N(pyridyl)$_2$	38	6	0.012	0.042	0.018	3.0×10^{-8}	3.6×10^{-8}
N(phenyl)$_2$	26	3	0.019		0.035	1.0×10^{-6}	
OMe	31	12	0.029	0.042	0.042	8.4×10^{-7}	1.0×10^{-6}
N(methyl)$_2$					0.068	1.4×10^{-4}	

in CN-Ph-N(phenyl)$_2$ decreases even further the conversion ratio to 29%. Even if the stability of photoisomers of CN-Ph-N(phenyl)$_2$ and CN-Ph-OMe is similar, the latter shows a higher conversion ratio of 43%. Once again, this result is due to the fact that the contribution of the TC form for CN-Ph-OMe is less important (see Table 2).

Owing to the presence of two TC forms in the reaction mechanism, in the cases of the CN-Ph-R substituted molecules it was impossible to use the algorithm previously illustrated for CN-Ph-H to obtain the molar extinction coefficients and the quantitative absorption spectra of the TC isomers. In consequence, quantum yields $\phi_{CF\rightarrow TC}$ for the conversion of CF into TC could not be measured. Nevertheless, upon short-term UV irradiation followed by complete thermal decay we could follow the bleaching kinetics of the signal corresponding to the sum of the two TC isomers converting back to the starting material. The rate constant values of this thermal bleaching are influenced by the presence of the various substituents on one of the phenyl rings linked to the sp3 carbon atom (Fig. 9 and Table 3) and exhibit a trend that is similar to that observed for the thermal decay of the TT species.

Fluorescence studies. Given that the *N*-phenyl carbazole is a chromophore that exhibits fluorescence emission[42] and that photochromism usually takes place from the lowest excited singlet state, we explored the possible fluorescence emission upon UV excitation of the five molecules investigated. This analysis was carried out to ascertain a possible competition between these two pathways in the deactivation of the lowest singlet excited state. The molecules were excited at 340 nm, the same wavelength employed for the photochromic studies, and the integrated emission spectra were compared to that obtained with quinine sulphate, used as a standard, under the same experimental conditions. However, for all five molecules very weak and noisy emission spectra were recorded, with very low fluorescence quantum yields of the order of $\phi_F \approx 7 \times 10^{-4}$. Therefore, the possible detrimental contribution of fluorescence to the photochromic reaction can be neglected under our experimental conditions.

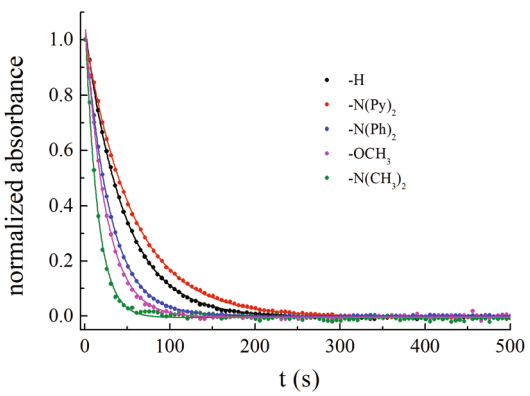

Fig. 9 Normalized decay kinetics of the TC isomers obtained after short-time UV irradiation of the five CN-Ph-R molecules.

Conclusions

In this paper, the photochromism of a series of newly synthesized *N*-phenyl carbazole benzopyrans has been investigated in toluene solution. The unsubstituted compound, CN-Ph-H, shows P-type photochromism, even though the TC form is more thermodynamically stable than the TT form, indicating that the photochromism is not always under thermodynamic control. In the present case, the P-type photochromism is obtained thanks to the steric hindrance provided by the phenyl group connected to the nitrogen on the diene part of TT forms, making the photo- and thermal-isomerisation more difficult.

The mechanism of the photochromic reaction, consisting of two consecutive steps where the TC and the TT coloured isomers are consecutively formed upon UV irradiation, has been elucidated. The spectrokinetic study allowed the estimation of most of the molar extinction coefficients, the quantum yields of visible photobleaching, and the rate constants of the fast and slow thermal bleaching processes.

In the case of the unsubstituted compound, CN-Ph-H, the quantum yield of UV photocolouration was also determined and an algorithm was used to obtain the complete quantitative absorption spectrum of the fast decaying TC isomer. For CN-Ph-H, the highest percentage of conversion (64%) of the initial chromene into the stable TT coloured isomer was measured, under our experimental conditions.

We investigated the effect of substituents with different donor strengths on one phenyl ring located at the 3-position on the spectrokinetic properties. While increasing the donor strengths shifts the absorption maximum of the photoproducts, the stability of TC and TT forms is decreasing. Reducing the stability of TC forms by two or four times, the stability of the corresponding TT forms is reduced by two- or four orders of magnitude, respectively. Interestingly, the elec-

tronic effects of *N*-diphenyl and methoxy groups on the stability of photoproducts are similar, while the *N*-diphenyl group leads to a significant shift of the absorption maximum. This *N*-diphenyl functionalisation at the 3-position could be interesting for the future design of naphthopyrans.

If on the one hand the unsubstituted compound CN-Ph-H and, to a lesser extent, also CN-Ph-N(pyridyl)$_2$, CN-Ph-N(phenyl)$_2$ and CN-Ph-OMe point towards a P-type photochromism, on the other hand CN-Ph-N(methyl)$_2$, functionalised with the strongest electron donating group, rather goes in the direction of a T-type photochromic compound. These results indicate the possibility to tune the type of photochromism from P-type to T-type by functionalisation. From this perspective, the effect of the substituent is of notable importance in providing some useful hints for the synthesis of new benzopyrans possessing long term stability of the TT coloured isomer(s) in the dark.

Conflicts of interest

There are no conflicts to declare.

Acknowledgements

F. O., A. Z. and D. P. gratefully acknowledge the financial support of the Ministero per l'Università e la Ricerca Scientifica e Tecnologica (Rome, Italy), the University of Perugia [PRIN 2010-2011, 2010FM738P], and the Istituto Nazionale di Fisica Nucleare (I.N.F.N.); M. M. and C. A. acknowledge financial support from JST ERATO Grant Number JPMJER1305, and JSPS KAKENHI Grant Number 19H02790; M. F. and J. M. acknowledge financial support from the Agence Nationale de la Recherche ANR-16-CE07-0024 (GATE). T. J.-O. acknowledges CNRS for a PhD grant.

References

1 B. Van Gemert, in *Organic Photochromic and Thermochromic Compounds*, ed. J. C. Crano and R. J. Guglielmetti, Kluwer Academic/Plenum Publishers, New York, 1999, vol. 1, pp. 111–140.
2 J. D. Hepworth and B. M. Heron, in *Functional Dyes*, ed. S.-H. Kim, Amsterdam, Elsevier, 2006, pp. 85–135.
3 N. S. Corns, S. M. Partington and A. D. Towns, Industrial organic photochromic dyes, *Color. Technol.*, 2009, **125**, 249–261.
4 J. Kolc and R. S. Becker, Proof of structure of the colored photoproducts of chromenes and spiropyrans, *J. Phys. Chem.*, 1967, **71**, 4045–4048.
5 C. Lenoble and R. S. Becker, Photophysics, photochemistry and kinetics of photochromic 2H-pyrans and chromenes, *J. Photochem.*, 1986, **33**, 187–197.
6 H. Bouas-Laurent and H. Dürr, Organic photochromism, *Pure Appl. Chem.*, 2001, **73**, 639–665.
7 G. Ottavi, G. Favaro and V. Malatesta, Spectrokinetic study of 2,2-diphenyl-5,6-benzo(2H)chromene: a thermoreversible and photoreversible photochromic system, *J. Photochem. Photobiol., A*, 1998, **115**, 123–128.
8 S. Delbaere, G. Vermeersch and J.-C. Micheau, Quantitative analysis of the dynamic behaviour of photochromic systems, *J. Photochem. Photobiol., C*, 2011, **12**, 74–105.
9 R. Demadrille, A. Rabourdin, M. Campredon and G. Giusti, Spectroscopic characterisation and photodegradation studies of photochromic spiro[fluorene-9,3′-[3′H]-naphtho[2,1-b]pyrans], *J. Photochem. Photobiol., A*, 2004, **168**, 143–152.
10 C. D. Gabbutt, M. Heron, A. C. Instone, S. B. Kolla, K. Mahajan, P. J. Coelho and L. M. Carvalho, Synthesis and photochromic properties of symmetrical aryl ether linked bi- and tri-naphthopyrans, *Dyes Pigm.*, 2008, **76**, 24–34.
11 R. S. Becker and J. Michl, Photochromism of Synthetic and Naturally Occurring 2H-Chromenes and 2H-Pyrans, *J. Am. Chem. Soc.*, 1966, **88**, 5931–5933.
12 B. Luccioni-Houze, M. Campredon, R. Guglielmetti and G. Giusti, Kinetic Analysis of Fluoro-[2 h]-Chromenes at the Photostationary States, *Mol. Cryst. Liq. Cryst.*, 1997, **297**, 161–165.
13 J. J. Luthem, The Effect of Substituents on the Ring Closure Reaction of Photo Activated Diarylnaphthopyrans, *Mol. Cryst. Liq. Cryst.*, 1997, **297**, 155–160.
14 A. Kumar, The Relationship Between the Structure and the Absorption Spectra of Naphtho[2,1-B]pyran, *Mol. Cryst. Liq. Cryst.*, 1997, **297**, 139–145.
15 J. Hobley, V. Malatesta, R. Millini, W. Giroldini, L. Wis, M. Goto, M. Kishimotoa and H. Fukumura, Photochromism of chromene crystals; a new property of old chromenes, *Chem. Commun.*, 2000, 1339–1340.
16 J. Aubard, F. Maurel, G. Buntinx, O. Poizat, G. Levi, R. Guglielmetti and A. Samat, Femto/Picosecond Transient Absorption Spectroscopy of Photochromic 3,3-Diphenylnaphtho[2,1-b]pyran, *Mol. Cryst. Liq. Cryst.*, 2000, **345**, 215–220.
17 S. Delbaere and G. Vermeersch, NMR characterization of allenyl-naphthol in the photochromic process of 3,3-diphenyl-[3H]-naphtho[2-1,b]pyran, *J. Photochem. Photobiol., A*, 2003, **159**, 227–232.
18 P. L. Gentili, E. Danilov, F. Ortica, M. A. J. Rodgers and G. Favaro, Dynamics of the excited states of chromenes studied by fast and ultrafast spectroscopies, *Photochem. Photobiol. Sci.*, 2004, **3**, 886–891.
19 R. G. Brown, M. Maafl, P. Foggi and L. Bussotti, The ultrafast dynamics of some photochromic naphthopyrans, in *Femtochemistry and Femtobiology*, ed. M. M. Martin and J. T. Hynes, 2004, 283–286.
20 F. Maurel, S. Lau Truong, J. P. Bertigny, R. Dubest, G. Lévi, J. Aubard, S. Delbaere and G. Vermeersch, SERS Study of 3,3-Diphenyl-naphtho[2,1-b]pyran: Another Evidence for Allenyl-Naphthol Involvement in the Photochromic Mechanism, *Mol. Cryst. Liq. Cryst.*, 2005, **430**, 235–241.
21 B. Moine, G. Buntinx, O. Poizat, J. Rehault, C. Moustrou and A. Samat, Transient absorption investigation of the

photophysical properties of new photochromic 3H-naphtho[2,1-b]pyran, *J. Phys. Org. Chem.*, 2007, **20**, 936–943.

22 B. Moine, J. Réhault, S. Aloïse, J.-C. Micheau, C. Moustrou, A. Samat, O. Poizat and G. Buntinx, Transient Absorption Studies of the Photochromic Behavior of 3H-Naphtho[2,1-b]pyrans Linked to Thiophene Oligomers via an Acetylenic Junction, *J. Phys. Chem. A*, 2008, **112**, 4719–4726.

23 J. Harada, K. Ueki, M. Anada, Y. Kawazoe and K. Ogawa, Solid-state Photochromism of Chromenes: Enhanced Photocoloration and Observation of Unstable Colored Species at Low Temperatures, *Chem. – Eur. J.*, 2011, **17**, 14111–14119.

24 T. T. Herzog, G. Ryseck, E. Ploetz and T. Cordes, The photochemical ring opening reaction of chromene as seen by transient absorption and fluorescence spectroscopy, *Photochem. Photobiol. Sci.*, 2013, **12**, 1202–1209.

25 Y. Inagaki, Y. Kobayashi, K. Mutoh and J. Abe, A Simple and Versatile Strategy for Rapid Color Fading and Intense Coloration of Photochromic Naphthopyran Families, *J. Am. Chem. Soc.*, 2017, **139**, 13429–13441.

26 S. Brazevic, S. Nizinski, R. Szabla, M. F. Rode and G. Burdzinski, Photochromic reaction in 3H-naphthopyrans studied by vibrational spectroscopy and quantum chemical calculations, *Phys. Chem. Chem. Phys.*, 2019, **21**, 11861–11870.

27 S. Brazevic, M. Baranowski, M. Sikorski, M. Rode and G. Burdzinski, Ultrafast dynamics of the transoid-cis isomer formed in photochromic reaction from 3H-naphthopyran, *ChemPhysChem*, 2020, **21**, 1402–1407.

28 C. M. Sousa, J. Berthet, S. Delbaere and P. J. Coelho, Synthesis of 1-Vinylidene-naphthofurans: A Thermally Reversible Photochromic System That Colors Only When Adsorbed on Silica Gel, *J. Org. Chem.*, 2013, **78**, 6956–6961.

29 C. Sousa, S. Saraiva, H. Macedo and P. Coelho, Grey colouring thermally reversible photochromic 1-vinylidene-naphthofurans, *Dyes Pigm.*, 2017, **141**, 269–276.

30 C. M. Sousa, J. Berthet, S. Delbaere, A. Polonia and P. J. Coelho, Control of the Switching Speed of Photochromic Naphthopyrans through Restriction of Double Bond Isomerization, *J. Org. Chem.*, 2017, **82**, 12028–12037.

31 C. M. Sousa and P. J. Coelho, Joining High Coloration and Fast Color Fading with Photochromic Fused-Naphthopyrans, *Eur. J. Org. Chem.*, 2020, 985–992.

32 H. Kuroiwa, Y. Inagaki, K. Mutoh and J. Abe, On-Demand Control of the Photochromic Properties of Naphthopyrans, *Adv. Mater.*, 2019, **31**, 1805661.

33 M. Frigoli, F. Maurel, J. Berthet, S. Delbaere, J. Marrot and M. M. Oliveira, The Control of Photochromism of [3H]-Naphthopyran Derivatives with Intramolecular CH-π Bonds, *Org. Lett.*, 2012, **14**, 4150–4153.

34 M. Frigoli, J. Marrot, P. L. Gentili, D. Jacquemin, M. Vagnini, D. Pannacci and F. Ortica, P-type Photochromism of new Helical Naphthopyrans: Synthesis, and Photochemical, Photophysical and Theoretical Study, *ChemPhysChem*, 2015, **16**, 2447–2458.

35 F. Ianni, S. Scorzoni, P. L. Gentili, A. Di Michele, M. Frigoli, E. Camaioni, F. Ortica and R. Sardella, Chiral separation of helical chromenes with chloromethyl phenylcarbamate polysaccharide-based stationary phases, *J. Sep. Sci.*, 2018, **41**, 1266–1273.

36 S. R. Meech and D. Phillips, Photophysics of some common fluorescence standards, *J. Photochem.*, 1983, **23**, 193–217.

37 M. M. Oliveira, M. A. Salvador, P. J. Coelho and L. M. Carvalho, New benzopyranocarbazoles: synthesis and photochromic behavior, *Tetrahedron*, 2005, **61**, 1681–1691.

38 J. C. Antilla, A. Klapars and S. L. Buchwald, The Copper-Catalyzed N-Arylation of Indoles, *J. Am. Chem. Soc.*, 2002, **124**, 11684–11688.

39 J. Pang, Y. Tao, S. Freiberg, X.-P. Yang, M. D'Iorioa and S. Wang, Syntheses, structures, and electroluminescence of new blue luminescent star-shaped compounds based on 1,3,5-triazine and 1,3,5-trisubstituted benzene, *J. Mater. Chem.*, 2002, **12**, 206–212.

40 M. M. Oliveira, M. A. Salvador, S. Delbaere, J. Berthet, G. Vermeersch, J. C. Micheau, P. J. Coelho and L. M. Carvalho, Remarkable thermally stable open forms of photochromic new N-substituted benzopyranocarbazoles, *J. Photochem. Photobiol., A*, 2008, **198**, 242–249.

41 P. R. Andrews, S. L. A. Munro, M. Sadek and M. G. Wong, The hybridization state of nitrogen as a conformational variable in biologically active molecules, *J. Chem. Soc., Perkin Trans. 2*, 1988, 711–718.

42 I. B. Berlman, *Handbook of fluorescence spectra of aromatic molecules*, Academic Press, 1971, p. 213.